A Comparison between Growth Morphology of "Eutectic" Cells/Dendrites and Single-Phase Cells/Dendrites

S.N. TEWARI, S.V. RAJ, and I.E. LOCCI

Directionally solidified (DS) intermetallic and ceramic-based eutectic alloys with an *in-situ* composite microstructure containing finely distributed, long aspect ratio, fiber, or plate reinforcements are being seriously examined for several advanced aero-propulsion applications. In designing these alloys, additional solutes need to be added to the base eutectic composition in order to improve their high-temperature strength, and provide for adequate toughness and resistance to environmental degradation. Solute addition, however, promotes instability at the planar liquid-solid interface resulting in the formation of two-phase eutectic "colonies."[1–4] Because morphology of eutectic colonies is very similar to the single-phase cells and dendrites, the stability analysis of Mullins and Sekerka[5] has been extended to describe their formation.[6,7,8] Onset of their formation shows a good agreement with this approach;[9] however, unlike the single-phase cells and dendrites, there is limited examination of their growth speed dependence of spacing, morphology, and spatial distribution.[4,10–11] The purpose of this study is to compare the growth speed dependence of the morphology, spacing, and spatial distribution of eutectic cells and dendrites with that for the single-phase cells and dendrites.

Figure 1 shows typical transverse (normal to the growth direction) and longitudinal microstructures of two-phase eutectic cells (Figure 1(a)) and dendrites (Figure 1(b)) in directionally solidified (DS) NiAl-Cr(3 pct Mo) samples solidified at 100 K cm^{-1}.[10] The alloy growth direction is indicated by the arrows in the corresponding longitudinal views at the bottom. The two-phase eutectic contrast within the eutectic colonies is not visible in these figures because of the low magnification. It is, however, evident in the typical high-magnification views of the colony boundary shown in the insets of the transverse micrographs. At growth speeds less than 3.5 $\mu m\ s^{-1}$, the microstructure (not shown here) was planar. It became cellular at higher growth speeds, as shown in Figure 1(a), for a sample grown at 7 $\mu m\ s^{-1}$. The longitudinal and transverse appearances of these eutectic cells are almost identical to the single-phase cells that form during directional solidification of binary alloys. At 35 $\mu m\ s^{-1}$ or higher growth speeds, the two-phase eutectic colonies developed a branched appearance, as shown in the longitudinal view of a sample directionally solidified at 70 $\mu m\ s^{-1}$ (Figure 1(b)). Faint trace of these branched features can also be seen within the corresponding transverse view at the top. However, these eutectic dendrites do not have the usual four-fold symmetry of the side branches associated with the liquid-solid interfacial energy anisotropy in the fcc single-phase dendrites. Instead, the two-phase eutectic dendrites have "seaweed type" branches very similar to those observed in the succinonitrile-acetone[12] at a very low degree of constitutional supercooling.

Assuming that the centers of mass of these eutectic cells and dendrites on the transverse views represent their locations, one can obtain *Voronoi polygons*, typical as shown in Figure 2(a) for the sample grown at 70 $\mu m\ s^{-1}$. The number within each polygon indicates the number of corresponding nearest neighbors. Figure 2(b) shows the relative frequency distribution of the number of nearest neighbors for the eutectic cells and dendrites in DS NiAl-Cr(3 pct Mo) samples directionally solidified at speeds ranging from 7 to 141 $\mu m\ s^{-1}$. There is no significant difference between the eutectic cells growing at speeds less than 70 $\mu m\ s^{-1}$ and the eutectic dendrites growing at higher speeds. A

S.N. TEWARI, Professor, is with the Chemical and Biomedical Engineering Department, Cleveland State University, Cleveland, OH 44115. Contact e-mail: s.tewari@csuohio.edu S.V. RAJ, Materials Research Engineer, and I.E. LOCCI, Principal Researcher, are with the Case Western Reserve University at the NASA-Glenn Research Center at Lewis Field, Cleveland, OH 44135.

Manuscript submitted September 11, 2003.

U.S. GOVERNMENT WORK NOT PROTECTED BY U.S. COPYRIGHT

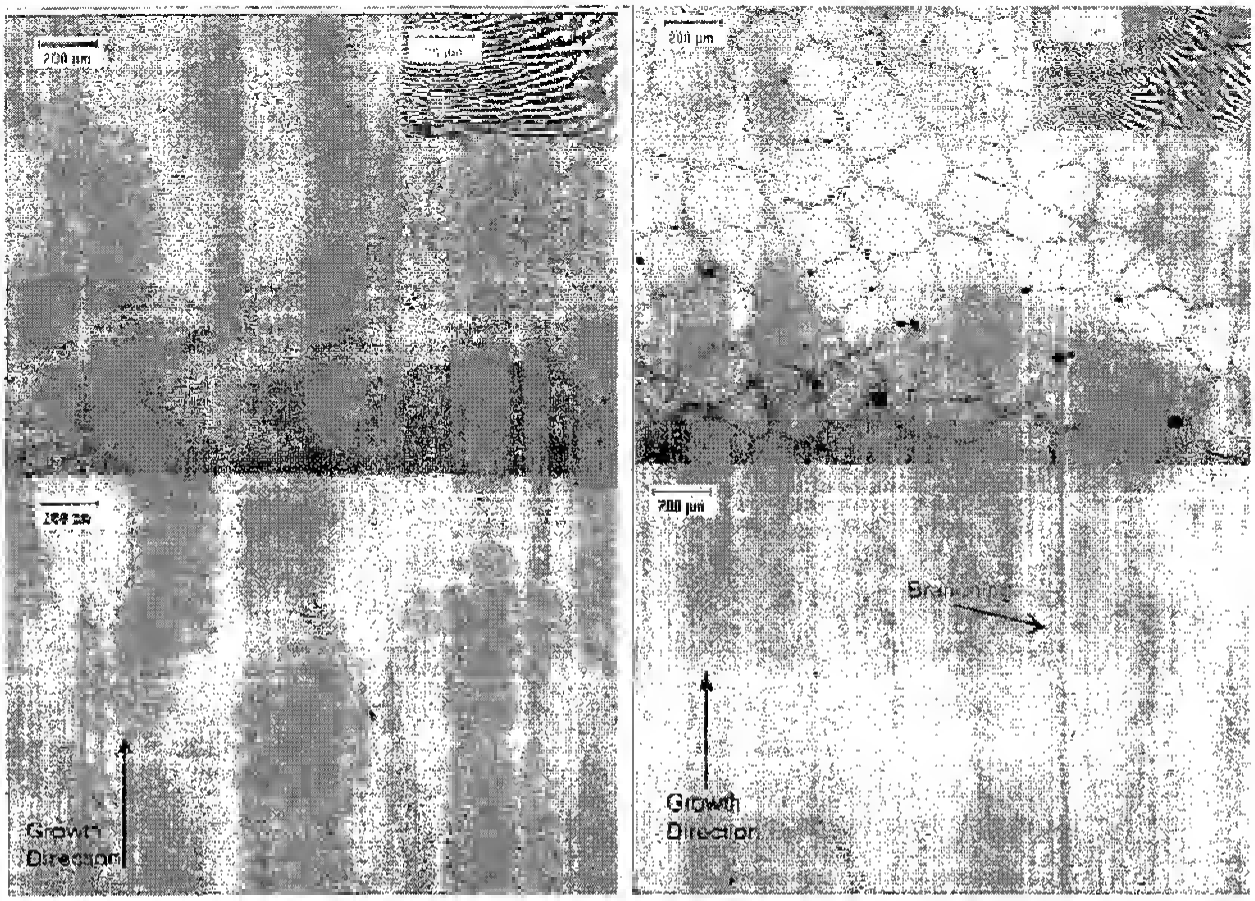

(*a*) (*b*)

Fig. 1—Typical transverse (shown at the top) and longitudinal (shown at the bottom) microstructures of (*a*) eutectic cells and (*b*) dendrites in DS NiAl-Cr(3 pct Mo) samples solidified at 100 K cm^{-1}. Arrows in the longitudinal views at the bottom show the alloy growth direction: (a) eutectic cells growing at 7 μm s^{-1} and (b) eutectic dendrites growing at 70 μm s^{-1}.

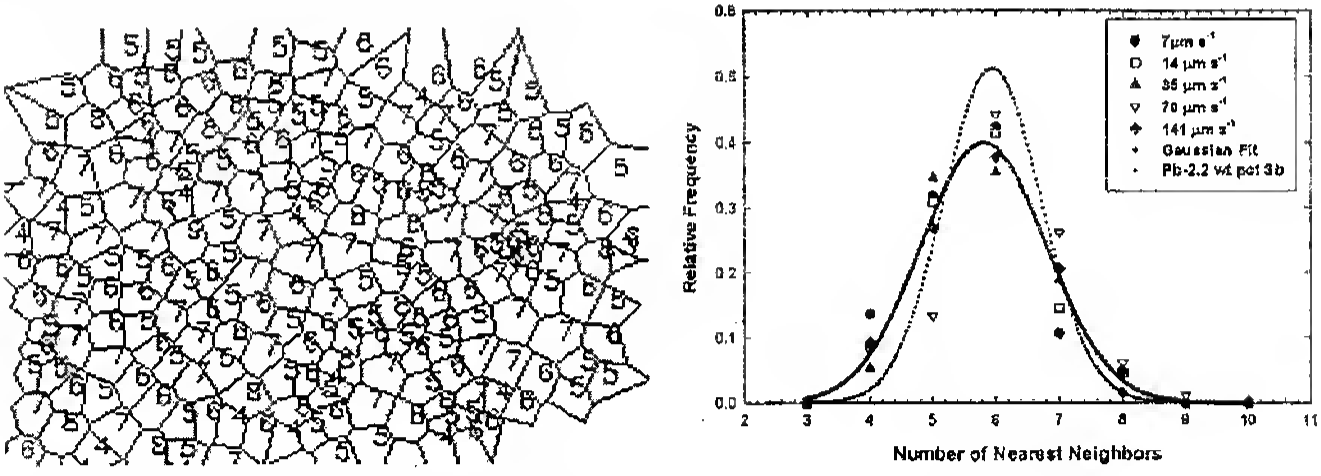

(*a*) (*b*)

Fig. 2—Spatial distribution of nearest neighbor eutectic cells and dendrites. (*a*) Voronoi polygons corresponding to the transverse microstructure shown in (b). (*b*) Frequency distribution of number of nearest neighbor eutectic cells and dendrites. Growth speeds for NiAl-Cr(3 pct Mo) alloy samples are indicated by the various symbols. The thick solid line is Gaussian fit to all the data points in (b). The thin broken line represents the Gaussian fit observed for the single-phase cells in DS Pb-2.2 wt pct Sb alloy.[13]

Gaussian fit through the data points, indicated by the solid line in Figure 2(b), shows that there is a dominance of five to six neighbors, but there is extensive noise embedded in the distribution. This behavior is very similar to that observed for the single-phase cells and dendrites in the fcc metallic alloys. However, the distribution of single-phase cells,

typically represented by that observed in DS Pb-2.2 wt pct Sb alloy[13] and included here as the dotted curve in Figure 2(b), is less noisy than that of eutectic cells.

Figure 3(a) shows the *minimum spanning tree* for the sample grown at 70 μm s^{-1}. A minimum spanning tree is a connected graph without any closed loop, which contains all the centers of mass of all the colonies and for which the sum of the edge lengths is minimal. Such a tree represents the shortest total length of the branches in order to connect all the nodes. The mean branch length (λ_1) and its standard deviation are a measure of the intercellular/interdendritic spacing. The mean branch length and its standard deviation can be normalized by dividing them by the square root of the average cell surface area to yield m and σ parameters. The m *vs* σ plots can then be used to compare arrangements with different nearest neighbor spacings.[14] Figure 3(b) plots the m and σ values obtained for the eutectic cell (at growth speeds less than 35 μm s^{-1}) and dendrite samples examined in this study (filled symbols). The open circles are for single-phase cells observed in DS Pb-2.2 wt pct Sb alloy samples.[13] The solid line in this figure corresponds to the expected m and σ values for a hexagonal tessellation with varying amounts of superimposed noise; the points on the solid line correspond to 10 pct noise increments starting from zero at $\sigma = 0$. As the imposed noise increases, the value of m decreases and that of σ increases. Figure 3(b) shows that the extent of disorder in the spacing distribution of eutectic cells and dendrites is generally higher than that observed in the single-phase cells; this is also in agreement with Figure 2(b), which showed that the frequency distribution of nearest neighbors is noisier for the eutectic cells/dendrites as compared with single-phase cells. This plot also shows that the extent of disorder increases with increasing growth speed; the branched eutectic features grown at speeds of 35 μm s^{-1} are more disordered as compared with the eutectic cells growing at lower growth speed.

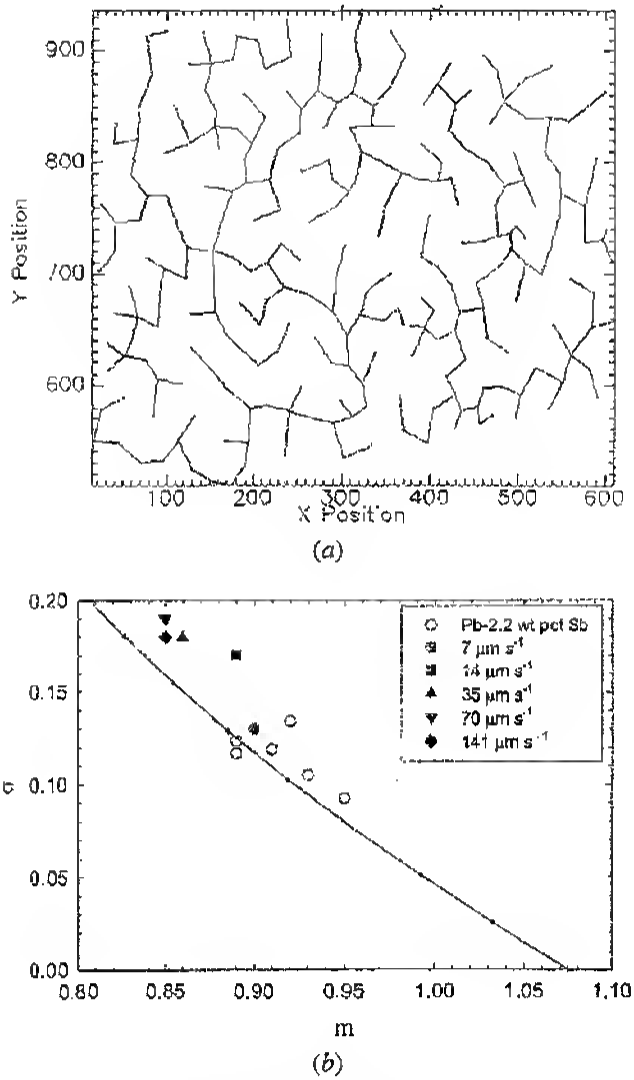

Fig. 3—Nearest neighbor spacing distribution of eutectic cells/dendrites in DS NiAl-Cr(3 pct Mo) alloy. (*a*) A minimum spanning tree based on the eutectic dendrite microstructure shown in Fig. 1(b). (*b*) The m-σ plot for the eutectic cells and dendrites observed in DS NiAl-Cr(3 pct Mo) alloy samples. The open circles correspond to the single-phase cells observed in the DS Pb-2.2 wt pct Sb alloy.[13] The solid line corresponds to a hexagonal tessellation with increasing amount of superimposed random noise generated by a uniformly distributed random-number generator. The points on the solid line correspond to noise increments of 10 pct starting from $\sigma = 0$.

Figure 4 plots the growth speed (V) dependence of the mean spacing (λ_1) of eutectic cells and dendrites and compares it with that of the single-phase cells. Mean cell/dendrite spacing and its standard deviation are plotted in Figure 4(a) as a function of growth speed for the DS NiAl-Cr(3 pct Mo) alloy. The regression fit (solid line in Figure 4(a)) shows the following dependence: $\lambda_1 = 358 \pm 60$ μm (V, μm s^{-1})$^{-0.19\pm0.05}$.

Figure 4(b) shows a schematic representation of the experimentally observed growth speed dependence of primary spacing for single-phase cells and dendrites. Shallow cells with almost spherical tips form at the onset of breakdown of a planar liquid-solid interface; their spacing decreases with increasing growth speed. At higher growth speed, deep cells with nearly elliptical tip shape form, resulting in an increase of spacing. The onset of side branching and formation of dendrites with paraboloidal tips cause a rapid spacing increase, resulting in the maximum shown in Figure 4(b). From then on, the spacing continues to decrease with increasing growth speed. It is quite evident that the growth speed dependence of the eutectic cells and dendrites (Figure 4(a)) is very different from that of single-phase cells and dendrites (Figure 4(b)). The spacing for the eutectic cells decreases with increasing growth speed, and it continues to decrease even after the formation of side branches as opposed to the rapid increase associated with the side-branch formation in the single-phase cells.

A power-law growth speed dependence, $\lambda_1 = AV^{-0.5}$, is predicted theoretically for single-phase cells.[15,16] As shown in Figure 4(c), this is in good agreement with experiments; Al-0.73 wt pct Cu[17] yields an exponent of -0.48, and succinonitrile-0.055 wt pct acetone[18] shows it to be -0.50. The two-phase eutectic cells and dendrites, however, yield a much lower exponent, about -0.19 for the NiAl-Cr(3 pct Mo) alloy examined here and -0.26 for the CBr_4-C_2Cl_6 eutectic alloy studied by Akamatsu and Faivre.[11]

The preceding observations indicate that the growth mechanisms of two-phase eutectic cells and dendrites must

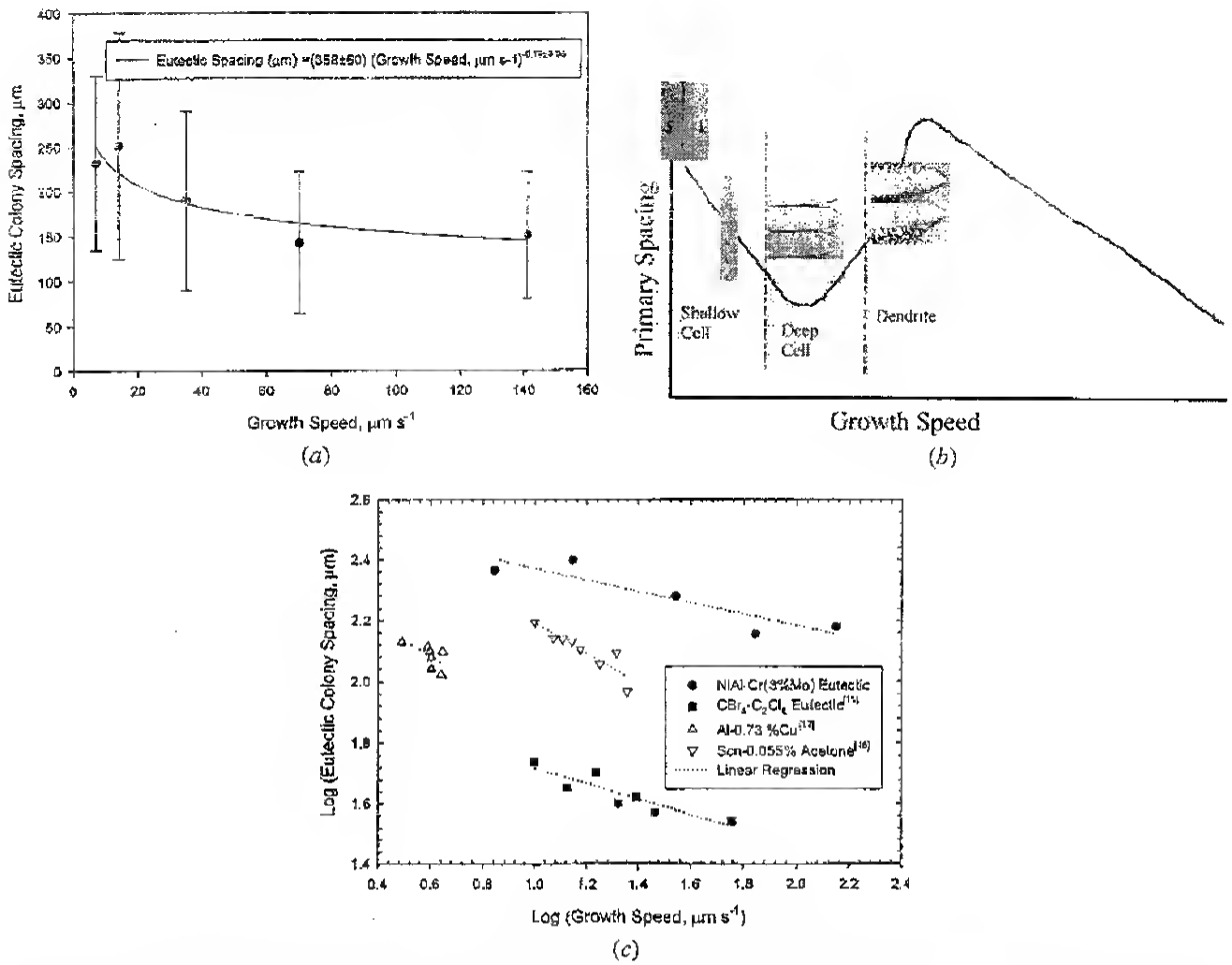

Fig. 4—A comparison between the growth speed dependence of eutectic cell and dendrite spacing with that of single-phase cells and dendrites. (*a*) Eutectic cells and dendrites in DS NiAl-Cr(3 pct Mo) alloy. (*b*) Single-phase cells and dendrites in DS binary alloys. (*c*) A comparison between growth speed dependence of eutectic cells and dendrites and that of single-phase cells during directional solidification.

be very different from those of the single-phase cells and dendrites.

Further theoretical development is needed to quantitatively predict growth speed dependence of morphology and spacing of the two-phase eutectic cells and dendrites.

REFERENCES

1. M.D. Rinaldi, R.M. Sharp, and M.C. Flemings: *Metall. Trans.*, 1972, vol. 3, pp. 3133-38 and pp. 3139-48.
2. M.F. Gell and H.W. Kerr: *Metall. Trans.*, 1972, vol. 3, pp. 2002-04.
3. D.J.S. Cooksey, D. Munson, M.P. Wilkinson, and A. Hellawell: *Phil. Mag.*, 1964, vol. 10, pp. 745-69.
4. W.M. Rumball: *Metallurgia*, 1968, vol. 78, pp. 141-45.
5. W.W. Mulins and R.F. Sekerka: *J. Appl. Phys.*, 1964, vol. 35, pp. 444-49.
6. H.E. Cline: *J. Appl. Phys.*, 1979, vol. 50 (7), pp. 4780-85.
7. J.S. Langer: *Phys. Rev. Lett.*, 1980, vol. 44, pp. 1023-26.
8. A. Karma and A. Sarkissan: *Metall. Mater. Trans. A*, 1996, vol. 27A, pp. 635-56.
9. M. Plapp and A. Karma: *Phys. Rev.*, 1999, vol. E60 (6), pp. 6865-89.
10. S.V. Raj and I.E. Locci: *Intermetallics*, 2001, vol. 9, pp. 217-27.
11. S. Akamatsu and G. Faivre: *Phys. Rev.*, 2000, vol. 61E (4), pp. 3757-70.
12. H. Song and S.N. Tewari: *Metall. Mater. Trans. A*, 1996, vol. 27A, pp. 1191-99.
13. S.N. Tewari, Y-Hsuan Weng, G.L. Ding, and R. Trivedi: *Metall. Mater. Trans. A*, 2002, vol. 33A, pp. 1229-43.
14. B. Billia, H. Jamgotchian, and H. Nguyen Thi: *Metall. Trans. A*, 1991, vol. 22A, pp. 3041-50.
15. J.D. Hunt: in *Solidification and Casting of Metals*, The Metals Society, London, 1979, Book 192, pp. 3-9.
16. J.D. Hunt and S.Z. Lu: *Metall. Mater. Trans. A*, 1996, vol. 27A, pp. 611-23.
17. G. Grange, J. Gastaldi, C. Jourdan, and B. Billia: *J. Cryst. Growth*, 1995, vol. 151, pp. 192-99.
18. S.H. Han and R. Trivedi: *Acta Metall. Mater.*, 1994, vol. 42 (1), pp. 25-41.